Vol. 11, No. 1 (2022) 73-86, DOI: 10.24874/ti.1052.02.21.05

Tribology in Industry

www.tribology.rs

RESEARCH

# Gravimetric, Electrochemical and Theoretical Study on Corrosion of AA6061/3wt% SiC/3wt% $B_4C$ Hybrid Composite in Acid Medium Using EDTA

Juan David Escobar Robledo[a], Prakasha Shetty[a,*], P. Preethi Kumari[a], M.C. Gowri Shankar[b], Sneha Kagatikar[a]

[a]*Department of Chemistry, Manipal Institute of Technology, Manipal Academy of Higher Education, Manipal-576104, Karnataka, India,*
[b]*Department of Mechanical and Manufacturing Engineering, Manipal Institute of Technology, Manipal Academy of Higher Education, Manipal-576104, Karnataka, India.*

Keywords:

*AA6061 hybrid composite*
*Corrosion inhibition*
*Potentiodynamic*
*Surface study*
*EDTA*

* Corresponding author:

*Prakasha Shetty*
*E-mail: prakash.shetty@manipal.edu*

*Received: 4 February 2021*
*Revised: 24 March 2021*
*Accepted: 14 May 2021*

A B S T R A C T

*The corrosion behaviour of Al6061/3wt%SiC/3wt%$B_4C$ hybrid composite was investigated in the presence of 0.5M HCl medium using gravimetric, electrochemical, and theoretical methods. In the present work, ethylenediaminetetraacetic acid disodium (EDTA) was used as an eco-friendly inhibitor. EDTA showed mixed inhibitor behavior, and its inhibition performance decreased with rising temperature from 303 to 323 K. EDTA evinced maximum inhibition efficiency of 82 % at 1.074 mM. The kinetic and thermodynamic results controlling corrosion were evaluated. The inhibition process occurred through the adsorption of EDTA on the hybrid composite sample, which obeyed Langmuir's adsorption isotherm. The experimental results were validated by theoretical study. The corroded and inhibited specimen's surface analysis performed using scanning electron microscopy (SEM) and atomic force microscopy (AFM) confirmed the adsorption of EDTA on the hybrid composite surface.*



## 1. INTRODUCTION

The two phases that are chemically non-reactive, the matrix and reinforcing, constitute a composite material. In composites' manufacture, the reinforcing grades used are particles, fibers, or flakes. In a composite material, the reinforcing phase embedded in the matrix phase. The reinforcing phase is usually less ductile compared to the matrix phase. Different kinds of matrix phases such as metals (Metal matrix composites, MMCs), polymers (Polymer matrix composites, PMCs), Ceramic (Ceramic matrix composites, CMCs) can make the composite materials. They can also be grouped as Particulate, Fibrous, and Laminate composites based on the reinforcement phases involved [1]. Low density, high rigidity, strength, ease for molding into complex shapes, low coefficient of thermal expansion, better fatigue resistance, etc., are the crucial advantages of composite materials over traditional materials [2]. In the production of MMCs, aluminium and its alloys are the widely used matrix

phases. These MMCs are the key "engineered materials" employed in the automotive and aerospace industry. The addition of non-metallic materials such as SiC, $B_4C$, etc., will boost the base matrix's mechanical and tribological properties [2,3].

Among the different Al alloys, AA6061 alloy exhibits lesser weight with high machinability and hardness. Their ability to form a stable oxide layer when exposed to the atmosphere makes them corrosion-resistant [4]. Hence, they are helpful in various domestic and industrial applications. However, aluminium alloys suffer from the disadvantage of possessing a low strength-to-weight ratio. This problem leads to an easy crash of material on the application of high load. It may be controlled by incorporating particulate materials like SiC, $B_4C$, etc., into the aluminium alloy matrix [5,6]. However, SiC/$B_4C$ as reinforcement material creates additional problems of depletion of the aluminium oxide layer formed on the composite surface. It thus reduces the resistance of the composite towards corrosion in the aggressive medium [7,8]. In automobile and aircraft industries, hydrochloric acid is widely employed as pickling, chemical, and electrochemical etching agents for aluminium alloys/composites [9]. In Al alloy hybrid composite, the presence of SiC/$B_4C$ as reinforcing material leads to surface discontinuity, which generates a large number of active sites for corrosion [8,10]. It is necessary, in such situations, to check the excessive dissolution of the metal. Among the different combating methods for corrosion, the addition of inhibitors to the corrosive medium is the most straightforward and cost-effective approach. Hence, it becomes necessary to utilize efficient corrosion inhibitors [11]. A literature survey reveals that organic compounds with heteroatoms (O, N, and S) are the most efficient corrosion inhibitors [12]. The usage of eco-friendly corrosion inhibitors has gained a lot of importance in recent years [13,14]. Low-cost and nontoxic inhibitor compounds showing good inhibition efficiency are the most preferred.

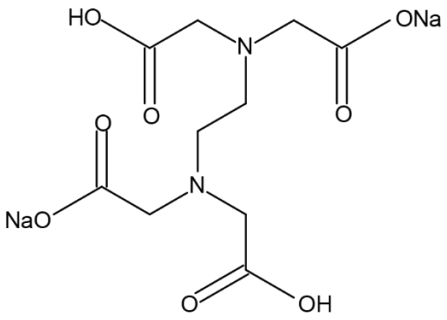


**Fig. 1.** The Structure of EDTA (disodium salt).

EDTA (Fig. 1) is an environmentally benign material that is readily soluble in the aqueous medium. Some of the other investigators used EDTA as the corrosion inhibitor for carbon steel [15] and Al [16]. The present work describes the experimental and theoretical study on combating AA6061/3wt% SiC/3wt% $B_4C$ hybrid composite corrosion in 0.5M HCl medium using EDTA as an inhibitor. Further, the experimental results obtained were supported by the theoretical as well as the surface morphological studies.

## 2. EXPERIMENTAL

### 2.1 Materials

A hybrid Al alloy composite, AA6061/3wt% SiC/3wt% $B_4C$, was employed as the study material in this work. The base matrix, AA6061 alloy used in this composite has the chemical composition (wt. %): 0.95 Mg; 0.52 Si; 0.55 Fe; 0.24 Cu; 0.14 Mn; 0.25 Cr; 97.35 Al. This alloy was reinforced with 3 wt% SiC and 3 wt% $B_4C$ particles [17]. In the gravimetric test, composite samples having 1cm diameter and 1cm thickness were used. A cylindrical test coupon of the hybrid composite was embedded in an acrylic resin material, leaving an exposed area of $1cm^2$. Initially, using emery papers of various grades (200-800), the specimen was abraded and then in a disc polisher with levigated alumina. Lastly, degreased using acetone, washed in distilled water, and dried. This specimen was employed in electrochemical studies. The stock solution of 0.5M HCl was prepared using an analytical grade sample of HCl (37 percent) and standardized by the volumetric method. EDTA disodium salt (Merck) was used as an inhibitor and its solution prepared in 0.5M HCl.

### 2.2 Gravimetric test

A freshly abraded test sample weighed accurately and then completely immersed in a100 ml of 0.5 M HCl solution without and with EDTA in a 250 ml beaker for 12h at 303K without stirring. A steady temperature of the test solution was maintained within ±1 K using a calibrated thermostat. Alter 12h of the immersion time; the specimen was removed from the test solution and immersed in nitric acid (70%) for 2-3 min to dissolve the corrosion product and then scrubbed the specimen surface with a bristle

brush in the presence of running water. Finally, the specimen was rinsed with acetone and dried [18]. The dried test specimen weighed again, calculated the corresponding weight loss, and repeated the same procedure at 24, 48, and 96 h of immersion time. Each measurement was carried out three times and used the mean value.

### 2.3 Electrochemical methods

Electrochemical studies were conducted using a workstation (USA model-CH604D series with beta software). A cell system consisting of a reference electrode (saturated calomel), an auxiliary electrode (platinum), and a working electrode (AA6061 hybrid composite) was employed. The experiments were conducted using a hybrid composite specimen embedded in acrylic resin with an exposed surface area, 1cm$^2$ and 0.5M HCl solution as the corrosive medium at three different temperatures (303, 313, and 323K) without and with the addition of inhibitor, EDTA. The temperature of the medium was maintained accurately (±1K) using a calibrated digital thermostat. A steady open circuit potential (OCP) was attained by submerging the working electrode in the test solution of 0.5 M HCl for 30 minutes.

In potentiodynamic polarisation (PDP) tests, the working electrode was polarised from −250 mV to +250 mV with a scan rate of 1mV/s at OCP. The Current vs. Potential plot (Tafel plot) was recorded. From the Tafel plot, corrosion potential ($E_{corr}$) and current density ($i_{corr}$) were obtained. Inhibition efficiencies were calculated by knowing the $i_{corr}$ corresponding to the blank and inhibited solution. Electrochemical impedance spectroscopy (EIS) tests were performed by applying an AC signal of 10 mV in 100 kHz-0.01 Hz frequency range at OCP. The Nyquist plot was recorded, and a suitable equivalent circuit was obtained using ZSimpwin software version 3.21.

### 2.4 Surface characterization

The surface morphological studies were conducted on AA6061 hybrid composite samples immersed for 3hrs in 0.5M HCl without and with EDTA. The surface images of specimens were recorded using SEM (EVO 18-5-57 model). The roughness of fresh, corroded and inhibited specimen surfaces were analyzed by AFM (IB342-Innova model).

### 2.5 Theoretical method

The quantum chemical measurements were performed with the aid of the software Gaussian Maestro material science suit with the correlation factor (B3LYP) and basis set (631+G) [19]. Highest occupied and lowest unoccupied molecular orbitals (HOMO and LUMO) obtained for EDTA were used to evaluate the parameters, such as the energies of HOMO ($E_{HOMO}$) and LUMO ($E_{LUMO}$), energy gap ($E_g$), etc.

## 3. RESULTS AND DISCUSSION

### 3.1. Gravimetric measurements

The weight loss was measured at different immersion times (12, 24, 48, and 96 h) at 303K by precisely weighing the composite samples before and after immersion in 100 ml of 0.5 M HCl and (0.5M HCl + EDTA) separately in a 250 ml beaker. In each case, the weight difference of the sample before and after immersion gives the weight loss.

The corrosion rate ($CR$) was computed from the Eq. (1) [20]:

$$CR = \frac{87.6\,W}{\rho A\,t}. \quad (1)$$

In this equation, W indicates the weight loss (g dm$^{-3}$), ρ represents the density (2.7 g cm$^{-3}$), and A the area (cm$^2$) of the composite sample, t indicates the immersion time (h).

The inhibition efficiency ($IE$) of EDTA in 0.5M HCl was obtained as per Eq. (2)[20]:

$$IE\ (\%) = \frac{W_0 - W}{W_0} \times 100. \quad (2)$$

In the above equation, $W_0$ and W indicate the weight loss of the composite samples immersed in 0.5 M HCl without and with EDTA, respectively, at 303 K.

The gravimetric measurements presented in Table 1 indicate the decrease in weight loss with an increase in the EDTA concentration in the acid medium. As a result, the $IE$ displayed by EDTA improved on increasing its concentration, and it has reached a maximum value of 83% at 1.074 mM EDTA. However, the weight loss obtained remains almost constant beyond this optimum EDTA concentration

(1.074 mM). As the EDTA concentration increases, the number of its molecules adsorbing on the composite surface also increased and reduced the active surface for the acid's attack on the composite body and increased *IE* of EDTA [20]. It is also evident from the gravimetric results that the *IE* of EDTA decreases marginally on raising specimen samples' immersion time from 12 to 96 h.

**Table 1**. The gravimetric test results for AA6061 hybrid composite in 0.5M HCl without and with EDTA at varied immersion time and 303 K.

| Immersion time (h) | [EDTA] (mM) | Wt. loss (mg) | CR (mmpy) | IE (%) |
|---|---|---|---|---|
| 12 | Blank | 11.5 | 4.024 | - |
| | 0.054 | 7.3 | 2.554 | 36.53 |
| | 0.107 | 5.7 | 1.995 | 50.42 |
| | 0.161 | 4.9 | 1.715 | 57.38 |
| | 0.215 | 3.7 | 1,294 | 67.84 |
| | 0.322 | 3.2 | 1.121 | 72.17 |
| | 0.537 | 2.4 | 0.840 | 79.13 |
| | 1.074 | 1.9 | 0.665 | 83.48 |
| 24 | Blank | 14.3 | 5.030 | - |
| | 0.054 | 9.3 | 3.272 | 34.96 |
| | 0.107 | 7.2 | 2.533 | 49.65 |
| | 0.161 | 6.3 | 2.216 | 55.94 |
| | 0.215 | 5.0 | 1.759 | 65.03 |
| | 0.322 | 4.5 | 1.583 | 68.53 |
| | 0.537 | 3.7 | 1.266 | 74.82 |
| | 1.074 | 2.6 | 0.914 | 81.82 |
| 48 | Blank | 21.0 | 7.545 | - |
| | 0.054 | 14.5 | 4.905 | 30.95 |
| | 0.107 | 11.2 | 3.825 | 46.67 |
| | 0.161 | 9.9 | 3.297 | 52.86 |
| | 0.215 | 7.9 | 2.588 | 62.38 |
| | 0.322 | 7.3 | 2.271 | 65.24 |
| | 0.537 | 6.1 | 1.780 | 70.95 |
| | 1.074 | 4.1 | 1.401 | 80.47 |
| 96 | Blank | 35.1 | 12.575 | - |
| | 0.054 | 27.0 | 9.674 | 23.07 |
| | 0.107 | 21.8 | 7.810 | 37.89 |
| | 0.161 | 20.3 | 7.273 | 42.16 |
| | 0.215 | 17.0 | 6.090 | 51.57 |
| | 0.322 | 14.2 | 5.375 | 59.54 |
| | 0.537 | 11.2 | 4.013 | 68.09 |
| | 1.074 | 7.4 | 2.651 | 78.92 |

### 3.2 PDP measurements

The corrosion inhibition behavior of EDTA on AA6061hybrid composite was tested using the PDP technique. As shown in Fig. 2, the hybrid composite's corrosion behavior in 0.5 M HCl and 0.5M HCl containing EDTA at 303 K represented as Tafel polarization curves. The *CR* of the hybrid composite and *IE* of EDTA have determined by Eq. (3) and (4) respectively [21]:

$$CR(\text{mmpy}) = \frac{3270 \times \text{M} \times i_{corr}}{\rho \times \text{Z}}. \quad (3)$$

Where, conversion factor = 3270, $i_{corr}$ = current density ($Acm^{-2}$), M = atomic mass of Al (27), ⍰ = density of Al (2.7 g $cm^{-3}$), and Z = number of electrons transferred per atom, 3.

$$IE(\%) = \frac{i_{corr} - i_{corr(inh)}}{i_{corr}} \times 100. \quad (4)$$

Where, $i_{corr}$ indicates the corrosion current density in 0.5M HCl while $i_{corr(Inh)}$ in (0.5M HCl + EDTA).

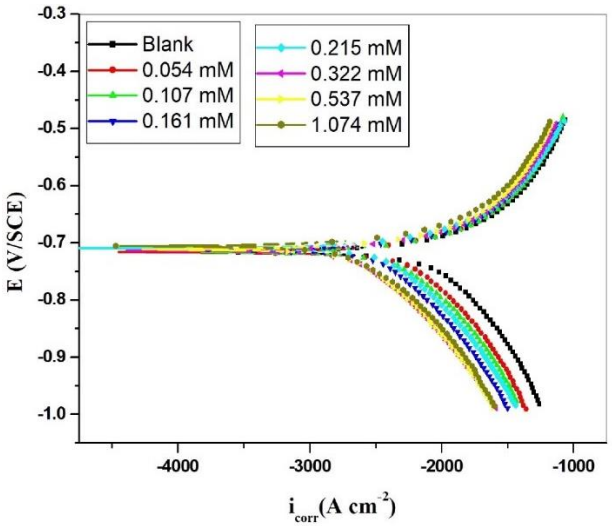


**Fig. 2.** Tafel plot for AA6061hybrid composite in 0.5M HCl without and with EDTA at 303 K.

It is clear from the PDP results (Table 2) that the *CR* of the hybrid composite exposed to the blank solution increased as the temperature increased. The blocking effect caused by the added EDTA to the acid medium resulted in a decrease in *CR* [22]. The efficiency of the inhibition improved with an increase in EDTA concentration. EDTA showed a moderate efficiency of 81.7% at 1.074 mM and 303K. Further, the *IE* of EDTA remains almost constant above 1.074mM EDTA concentration. The decrease in IE observed with a temperature increase indicates that EDTA molecules' adsorption occurs primarily through physisorption [23]. According to the literature, if the observed change of the $E_{corr}$ value in the inhibited medium is greater than ±85 mV compared to the corroded medium, the inhibitor may be regarded as cathodic or anodic [24]. The difference in $E_{corr}$ value obtained in the present case is less than 85mV, which supports the claim that EDTA functions as a mixed form inhibitor. It is evident (Table 2) that the addition of EDTA to

the acid medium has not caused a significant change in the cathodic slope ($b_c$) values, which suggests that the EDTA blocks the active sites on the hybrid composite surface without modifying the corrosion process mechanism [25].

**Table 2**. PDP results for AA6061 hybrid composite in 0.5M HCl without and with EDTA at varied temperatures.

| T (K) | [EDTA] (mM) | $E_{corr}$ (mV) | $b_c$ (mVdec$^{-1}$) | $i_{corr}$ (mAcm$^{-2}$) | CR (mmpy) | IE (%) |
|---|---|---|---|---|---|---|
| 303 | Blank | -702 | 50.50 | 5.850 | 2.515 | - |
| | 0.054 | -726 | 52.18 | 3.811 | 1.635 | 34.9 |
| | 0.107 | -727 | 54.21 | 2.971 | 1.275 | 49.2 |
| | 0.161 | -729 | 53.03 | 2.563 | 1.099 | 56.2 |
| | 0.215 | -729 | 53.17 | 1.778 | 0.863 | 65.7 |
| | 0.322 | -724 | 54.49 | 1.765 | 0.757 | 69.8 |
| | 0.537 | -710 | 53.97 | 1.384 | 0.593 | 76.3 |
| | 1.074 | -706 | 52.31 | 1.068 | 0.467 | 81.7 |
| 313 | Blank | -715 | 47.50 | 13.55 | 5.825 | - |
| | 0.054 | -719 | 45.37 | 11.02 | 4.728 | 18.7 |
| | 0.107 | -719 | 46.04 | 10.50 | 4.505 | 22.5 |
| | 0.161 | -715 | 45.44 | 8.972 | 3.848 | 33.8 |
| | 0.215 | -717 | 45.31 | 8.530 | 3.659 | 37.0 |
| | 0.322 | -730 | 50.68 | 6.792 | 2.914 | 49.9 |
| | 0.537 | -717 | 48.00 | 6.136 | 2.632 | 54.7 |
| | 1.074 | -713 | 48.43 | 5.195 | 2.228 | 61.7 |
| 323 | Blank | -725 | 45.50 | 17.30 | 7.410 | - |
| | 0.054 | -741 | 42.82 | 15.03 | 6.447 | 13.1 |
| | 0.107 | -727 | 44.90 | 13.97 | 5.989 | 19.2 |
| | 0.161 | -739 | 44.37 | 12.87 | 5.521 | 25.6 |
| | 0.215 | -734 | 44.80 | 11.70 | 5.019 | 32.4 |
| | 0.322 | -739 | 46.25 | 9.906 | 4.249 | 42.7 |
| | 0.537 | -738 | 47.33 | 9.285 | 3.983 | 46.3 |
| | 1.074 | -735 | 49.47 | 7.625 | 3.271 | 55.9 |

### 3.3 Effects of temperature

The PDP results (Table 2) indicate that the *IE* of EDTA decreases as the temperature increases, which may be due to higher temperature increasing dissolution rates of aluminium and the probable desorption of adsorbed EDTA molecules. The physisorption of EDTA over the composite surface indicates such behaviour [26, 27]. The activation parameters like activation energy ($E_a$), enthalpy ($\Delta H_a$), and entropy ($\Delta S_a$) of activations have measured using the experimental results on the corrosion of hybrid composite at varied temperatures. The Arrhenius equation [28] was used to calculate the $E_a$ value.

$$\ln(CR) = \mathrm{B} - \frac{\mathrm{E_a}}{\mathrm{RT}}. \qquad (5)$$

Where B indicates the Arrhenius constant in the above relation. R represents the universal gas constant, and T is the temperature (K).

Arrhenius plots (Fig. 3 (a)) indicate straight-line graphs with the correlation coefficient ($R^2$) value almost closer to unity (Table 3). From the straight-line slope (–Ea/R), the Ea value was computed. As per Table 3, the inhibited medium's $E_a$ values are more significant than that in the blank, which implies that the rate of deterioration of hybrid composite is under control. EDTA adsorption on the hybrid composite surface blocks the transfer of charge during the corrosion process, increasing Ea [29]. The Ea values increased on increasing the EDTA concentration, which supports the possibility of the physisorption of EDTA on the hybrid composite surface [30]. ΔHa and ΔSa values for the inhibition process was calculated from the transition state relation, Eq. (6) [31]:

$$\mathrm{CR} = \frac{\mathrm{RT}}{\mathrm{Nh}} \exp\left(\frac{\Delta S_a}{\mathrm{R}}\right) \exp\left(-\frac{\Delta \mathrm{H_a}}{\mathrm{RT}}\right). \qquad (6)$$

Where h is the Plank's constant and N is the Avogadro's number.

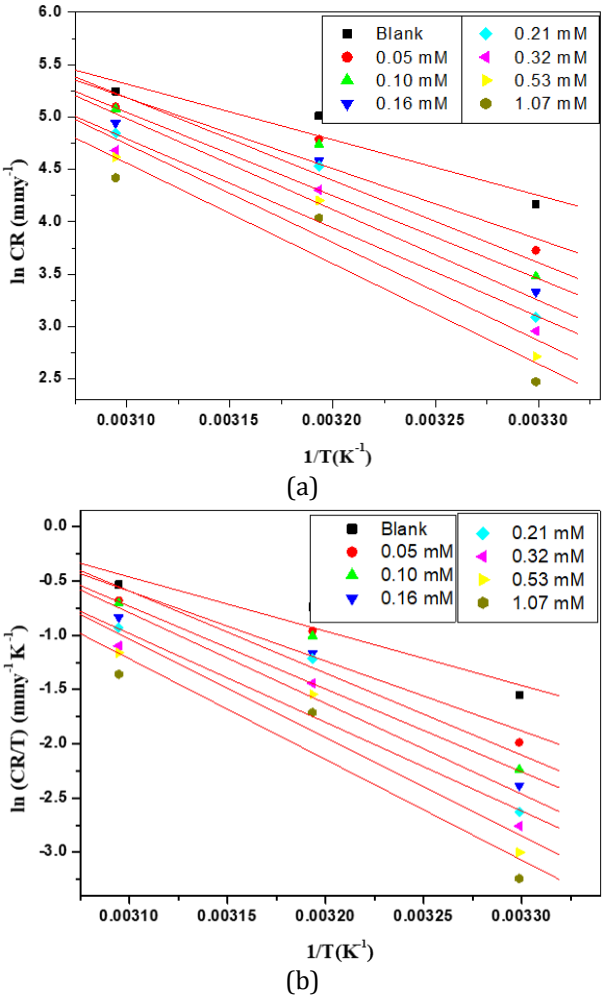


**Fig. 3.** (a) Arrhenius plot, and (b) ln(CR)/T vs. 1/T plot for AA6061 hybrid composite in 0.5 M HCl and (0.5M HCl + EDTA).

The ln(CR/T) vs. 1/T plot (Fig. 3. (b)) gave a straight-line. The correlation coefficient ($R^2$) of the plot obtained is almost closer to unity (Table 3). The recorded $\Delta H_a$ and $\Delta S_a$ values (Table 3) are computed from the slope given by $-\Delta H_a/R$ and the intercept by $[\ln(R/Nh) + \Delta S_a/R]$, respectively. In the inhibited medium, the $\Delta S_a$ values are more positive than in the blank medium, suggesting the development of an ordered, stable film of EDTA on the hybrid surface [32].

**Table 3**. Activation parameters for AA6061 hybrid composite in 0.5 M HCl without and with EDTA.

| [EDTA] (mM) | $E_a$ (KJmol$^{-1}$) | $R^2$ | $\Delta H_a$ (KJmol$^{-1}$) | $\Delta S_a$ (Jmol$^{-1}$K$^{-1}$) | $R^2$ |
|---|---|---|---|---|---|
| Blank | 44.21 | 0.9588 | 41.61 | -72.38 | 0.9514 |
| 0.054 | 56.18 | 0.9588 | 53.58 | -36.38 | 0.9548 |
| 0.107 | 65.50 | 0.9567 | 62.90 | -7.48 | 0.9504 |
| 0.161 | 66.10 | 0.9567 | 63.50 | -6.78 | 0.9547 |
| 0.215 | 72.18 | 0.9588 | 69.58 | 11.58 | 0.9401 |
| 0.322 | 70.65 | 0.9541 | 68.05 | 27.48 | 0.9533 |
| 0.537 | 77.97 | 0.9581 | 75.37 | 27.48 | 0.9533 |
| 1.074 | 79.76 | 0.9440 | 77.16 | 31.55 | 0.9466 |

### 3.4 Adsorption isotherm

We can analyse the possible interaction of EDTA at the AA6061 hybrid composite surface by applying the different adsorption isotherms to the system. The mechanism of inhibition can be better understood from the adsorption isotherm followed. Langmuir's adsorption isotherm [33] was obeyed more precisely in this case among the various adsorption isotherms examined. The adsorption isotherm of Langmuir's stated as

$$\frac{C_{inh}}{\theta} = \frac{1}{K_{ads}} + C_{inh}\,. \qquad (7)$$

In this equation, $C_{inh}$ = concentration of EDTA, and $K_{ads}$ = equilibrium constant for adsorption. The surface coverage ($\theta$) value was obtained using the Eq. (8):

$$\theta = \frac{\mathrm{IE}(\%)}{100}\,. \qquad (8)$$

The graph of $C_{inh}/\theta$ vs. $C_{inh}$ displayed a straight-line (Fig. 4 (a)) with the correlation coefficient ($R^2$) value closer to one (Table 4), which reveals that adsorption of EDTA followed Langmuir's isotherm model [14]. The straight-line plot intercept gives the value of $K_{ads}$, which was used as per the Eq. (9) to obtain the standard free energy of adsorption ($\Delta G^o_{ads}$) [34].

$$K_{\mathrm{ads}} = \frac{1}{55.5}\,\mathrm{e}\left(\frac{-\Delta G^{\circ}_{ads}}{\mathrm{RT}}\right). \qquad (9)$$

Where 55.5 indicates the concentration of water in solution (mol L$^{-1}$). The graph of $\Delta G^{\circ}_{ads}$ vs. T displayed a straight-line plot (Fig. 4 (b)). The entropy ($\Delta S^{\circ}_{ads}$) and enthalpy ($\Delta H^{\circ}_{ads}$) of adsorption values have computed using the slope and intercept values of the straight-line plot (Fig. 4 (b)) as per the Eq. (10):

$$\Delta G^{0}{}_{ads} = \Delta H^{0}_{ads} - T\Delta S^{0}_{ads}\,. \qquad (10)$$

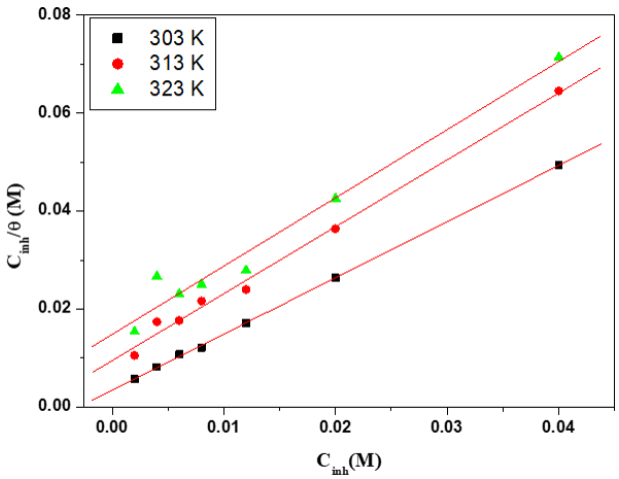


(a)

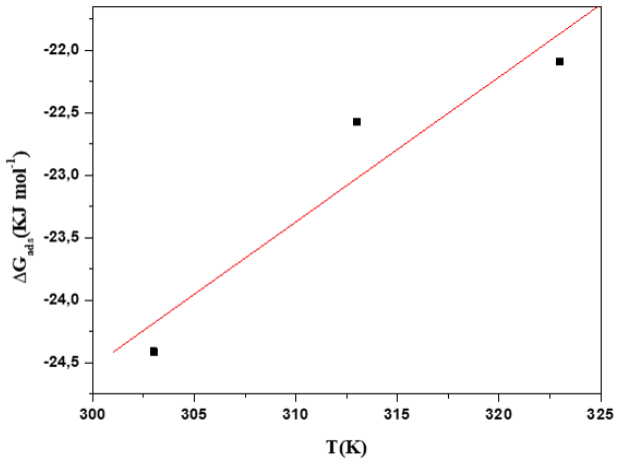


(b)

**Fig. 4.** (a) Langmuir adsorption isotherm and (b) $\Delta G^{\circ}_{ads}$ vs. T plots for the adsorption of EDTA from 0.5M HCl on the hybrid composite.

**Table 4**. The thermodynamic results for EDTA adsorption on AA6061 hybrid composite in 0.5M HCl.

| T (K) | $\Delta G_{ads}$ (KJmol$^{-1}$) | Slope | $R^2$ | $\Delta H^{o}_{ads}$ (KJ mol$^{-1}$) | $\Delta S^{o}_{ads}$ (Jmol$^{-1}$K$^{-1}$) |
|---|---|---|---|---|---|
| **303** | -24.41 | 1.147 | 0.9472 | -59.33 | 0.116 |
| **313** | -22.57 | 1.136 | | | |
| **323** | -22.09 | 1.393 | | | |

The thermodynamic measurements have displayed in Table 4. According to the literature, the $\Delta G^{o}_{ads}$ value up to -20kJmol$^{-1}$

implies physisorption while greater than -40kJmol$^{-1}$ implies chemisorption [35]. In the present case, the obtained $\Delta G^{o}_{ads}$ values lie between -20 and -40 kJmol$^{-1}$ and closer to 20 kJmol$^{-1}$, which indicates that EDTA adsorption on the composite surface occurs through mixed adsorption, mainly with physisorption. The negative value of $\Delta H^{o}_{ads}$ also suggests the possibility of the physisorption of EDTA on the hybrid composite [35]. The $\Delta S^{o}_{ads}$ value is positive, which shows that the randomness induced due to water displacement from the hybrid composite surface exceeds the reduction in entropy due to the organized arrangement of EDTA molecules on the hybrid composite surface [36].

### 3.5 EIS measurements

Nyquist plots depicting the corrosion behaviour of AA6061 hybrid composite in 0.5M HCl without and with EDTA are shown in Fig. 5 (a). The semi-circular nature of Nyquist plots recorded indicates that corrosion is a charge transfer controlled process. The diameter of the semicircle plot increased on increasing the EDTA concentration. The increase in the capacitive loop diameter suggests that the presence of EDTA controls the charge transfer process [37]. The depressed semicircle plots obtained may be due to the hybrid composite's surface nature, such as roughness, impurity, grain boundaries, and distribution of active surface sites [38]. The impedance plots of a similar type were reported earlier for the corrosion of Al alloy/composite in HCl solution [39-41]. The EIS data obtained in the presence of EDTA was fitted into an equivalent circuit as shown in Fig. 5 (b) using the ZSimpWin software version 3.21. The equivalent circuit contains elements like charge transfer resistance ($R_{ct}$), the constant phase element ($Q$), the solution resistance ($R_s$), the inductance resistance ($R_L$), and the inductor ($L$). In the equivalent circuit, $Q$, $R_{ct}$, and $R_L$ are parallel, whereas $L$ and $R_L$ are in series. The polarisation resistance ($R_p$) was computed from Eq. (11) [39].

$$R_p = \frac{R_L\, R_{ct}}{R_L + R_{ct}}. \qquad (11)$$

The $C_{dl}$ (double layer capacitance) value was obtained using Eq. (12) [41].

$$C_{dl} = \frac{1}{2\pi R_P f_{max}}. \qquad (12)$$

Where $f_{max}$ is the frequency at which an imaginary part of impedance (–Z ″) shows the maximal value. The inhibition efficiency, $IE$ (%) of EDTA, was obtained using Eq. (13) [39].

$$IE\ (\%) = \frac{R_{p(inh)} - R_p}{R_{p(inh)}} \times 100\,. \qquad (13)$$

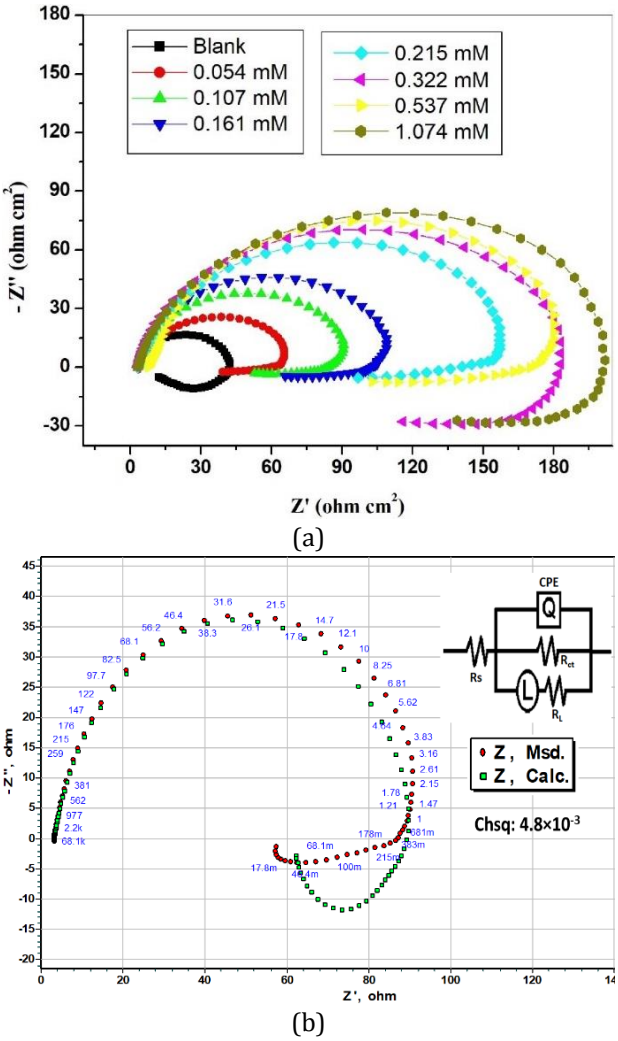


**Fig. 5.** (a) Nyquist plots for AA6061 hybrid composite in 0.5M HCl without and with EDTA at 303 K; (b)The equivalent circuit used to fit EIS data of AA6061 hybrid composite in 0.5M HCl containing 0.107mM EDTA at 303 K.

$R_p$ is the blank medium's polarisation resistance, and $R_{p(inh)}$ in the inhibited medium. $R_p$ values increased, whereas $C_{dl}$ decreased at a higher concentration of EDTA (Table 5). $R_p$ values observed increase might be due to the rise in the resistance offered by the adsorbed film of EDTA molecules towards the composite corrosion. A decrease in $C_{dl}$ observed on increasing EDTA concentration may be due to an increased thickness of the electric double layer at the composite/acid medium interface [41].

**Table 5**. EIS results for AA6061 hybrid composite in 0.5M HCl without and with EDTA.

| [EDTA] (mM) | $R_P$ (Ωcm²) | $C_{dl}$ (µF cm⁻²) | *IE* (%) |
|---|---|---|---|
| Blank | 37.1 | 262.6 | - |
| 0.054 | 58.5 | 73.58 | 36.2 |
| 0.107 | 77.36 | 52.54 | 52.2 |
| 0.161 | 85.25 | 39.77 | 56.5 |
| 0.215 | 115.1 | 21.53 | 67.8 |
| 0.322 | 130.5 | 16.68 | 71.5 |
| 0.537 | 176.5 | 11.71 | 79.0 |
| 1.074 | 201.2 | 9.90 | 81.6 |
| Blank | 28.5 | 742.2 | - |
| 0.054 | 35.5 | 339.0 | 19.7 |
| 0.107 | 40.2 | 262.2 | 29.1 |
| 0.161 | 43.5 | 221.7 | 34.5 |
| 0.215 | 49.3 | 152.9 | 42.2 |
| 0.322 | 55.1 | 110.9 | 48.3 |
| 0.537 | 64.8 | 81.11 | 56.0 |
| 1.074 | 85.8 | 41.64 | 66.8 |
| Blank | 10.5 | 4332 | - |
| 0.054 | 11.8 | 3331 | 11.0 |
| 0.107 | 13.21 | 2094 | 21.3 |
| 0.161 | 14.72 | 1444 | 29.3 |
| 0.215 | 16.15 | 969 | 35.6 |
| 0.322 | 17.76 | 667 | 41.4 |
| 0.537 | 19.21 | 571 | 45.9 |
| 1.074 | 25.02 | 366 | 58.4 |

### 3.6 Proposed corrosion inhibition mechanism

Generally, organic inhibitors either control metal/composite corrosion by physisorption, chemisorption, or mixed adsorption. Based on the corrosion reactions for aluminium in HCl medium, one can predict the inhibition mechanism involved. During the aluminium corrosion in HCl medium, the following reactions occur at anode [42]:

$$Al + Cl^- \rightleftharpoons AlCl^-_{ads} \quad (14)$$

$$AlCl^-_{ads} + Cl \longrightarrow AlCl^+_2 + 3e^- \quad (15)$$

Similarly, the possible cathode reaction includes the release of hydrogen gas, as indicated below.

$$H^+ + e^- \longrightarrow H_{ads} \quad (16)$$

$$H_{ads} + H_{ads} \longrightarrow H_2 \quad (17)$$

Generally, because of the electric field generated at the interface, the metal surface in contact with a solution is charged. The $pH_{Zch}$ value (i.e., the pH value corresponding to zero charge potential) for Al is equal to 9.1 [42]. Hence, aluminium acquires a positive charge in the highly acidic medium, similar to the one used in this work. As a result, the positively charged hybrid composite surface can attract the acid medium's chloride ions (Fig. 6). Thus, the net charge on the composite surface becomes negative. At very low pH or very acidic conditions, EDTA exists in a hexaprotic form, designated as $H_6Y^{2+}$ [43]. Physisorption occurs when the negatively charged hybrid composite surface attracts positively charged protonated EDTA (Fig. 6). The heteroatoms (N, O) and π bonds in EDTA can interact with Al atoms' vacant p-orbital on the composite surface, resulting in forming the coordination type bonds [44].

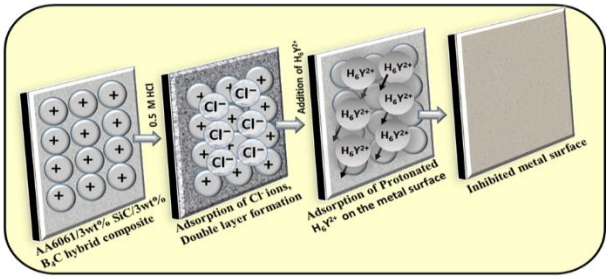


**Fig. 6.** Physisorption model for EDTA.

### 3.7 SEM Analysis

To find the effect of the presence of EDTA in the acid medium on the corrosion of AA6061 hybrid composite, we took the SEM pictures of the specimen surface. The SEM picture of the hybrid composite presented in Fig. 7 (a) shows a clean uniform surface of the freshly abraded composite specimen. However, Fig. 7 (b) shows deep pits formed because of the SIC/$B_4C$ particle's detachment from hybrid composite by the acid medium's aggressive attack. Micro galvanic corrosion at the interface between the reinforcing particle (cathodic area) and the matrix (anodic area) of the hybrid composite results in deep pits formation. The SEM image of the inhibited specimen sample (Fig. 7 (c)) showed a smooth surface with few holes. This indicates a drastic reduction in the acid medium's aggressive action due to the adsorption of EDTA on the hybrid composite resulting in the deposition of a defensive film.

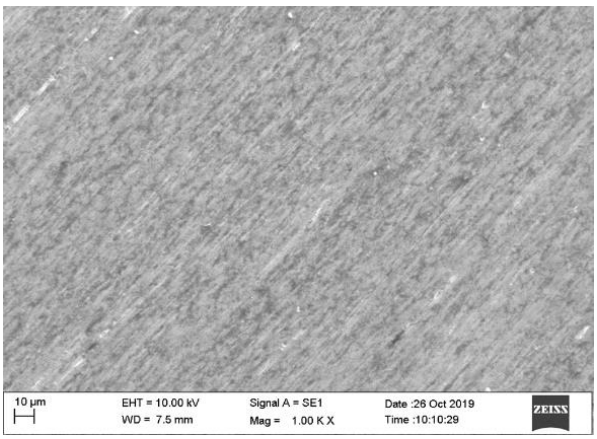


(a)

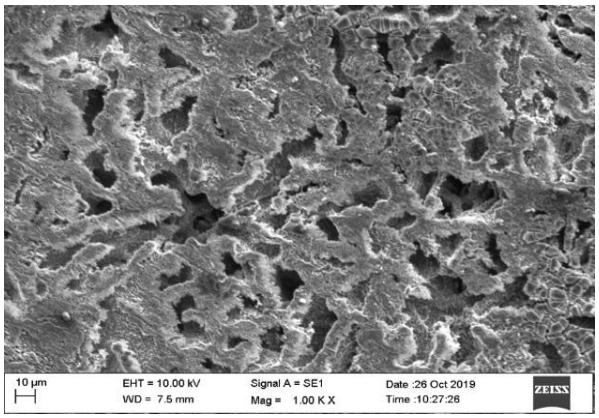


(b)

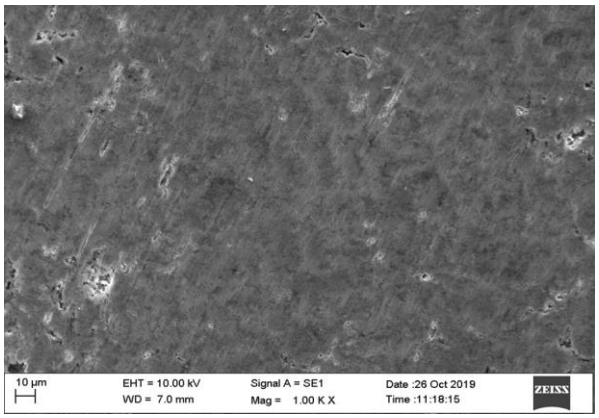


(c)

**Fig. 7.** SEM images of AA6061 hybrid composite specimen (a) freshly abraded; immersed in (b) 0.5 M HCl, and (c) (0.5M HCl +1.074mM EDTA).

### 3.8 AFM Analysis

The AFM images of AA6061 hybrid composite specimen freshly abraded and exposed to 0.5M HCl without and with 1.074mM EDTA are presented in Fig. 8 (a)-(c). The image of the inhibited specimen (Fig. 8 (c)) showed a smooth surface compared to the corroded one (Fig. 8 (b)). The surface roughness (Average roughness, $R_a$ and Root mean square roughness, $R_q$) values for the inhibited specimen are far less compared to the corroded one (Table 6). The low surface roughness values for the inhibited sample reveals the adsorption of EDTA and subsequent formation of protective film onto the hybrid composite surface. As a result, the corrosion of the hybrid composite specimen was controlled.

**Table 6.** AFM analysis results for AA6061 hybrid composite in 0.5M HCl without and with EDTA.

| AA 6061 hybrid composite specimen | $R_a$ (nm) | $R_q$ (nm) | $R_{max}$ (nm) |
|---|---|---|---|
| Freshly abraded | 37.3 | 49.4 | 660 |
| Exposed to 0.5 M HCl | 275 | 195 | 1850 |
| Exposed to (0.5M HCl + 1.074 mM EDTA) | 43 | 56.1 | 738 |

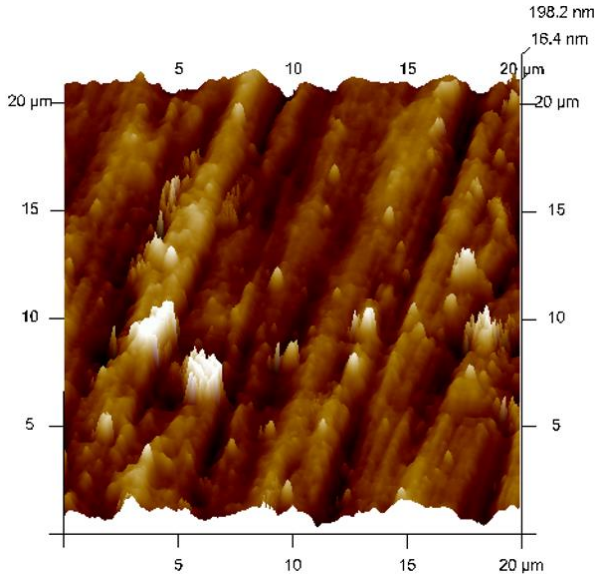


(a)

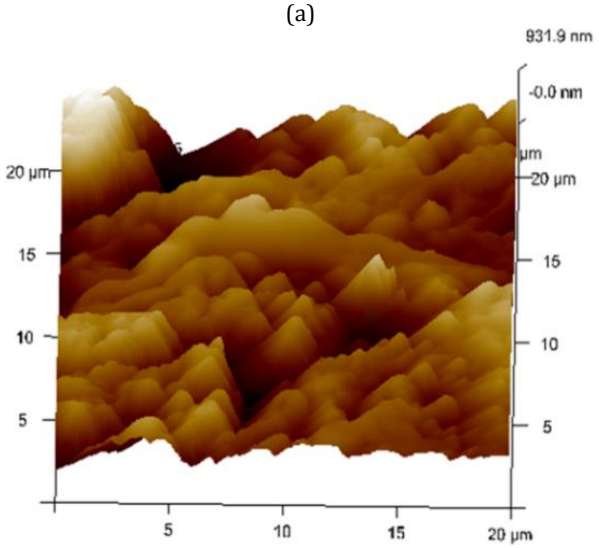


(b)

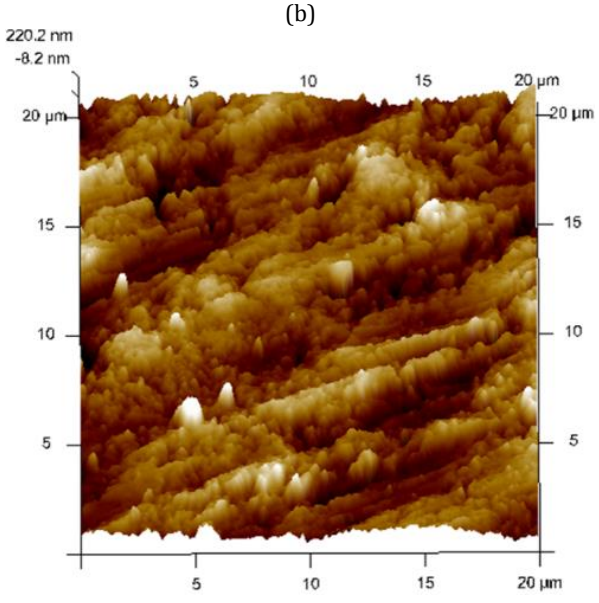


(c)

**Fig. 8.** AFM images of AA6061hybrid composite specimen (a) freshly abraded; immersed in (b) 0.5M HCl, and (c) (0.5M HCl + 1.074 mM EDTA).

### 3.9 Theoretical study

An organic inhibitor's corrosion combating properties are mainly related to its geometry and its HOMO and LUMO. In the current work, theoretical calculations were performed using Density Functional Theory (DFT) to understand the structure-inhibition activity relationship of EDTA. $E_{HOMO}$, $E_{LUMO}$, $E_g$ values, and the Mullikan's charges on the inhibitor molecule have been obtained from the theoretical study. Mullikan's charges help to identify the electron donor and acceptor centres in the inhibitor molecule. The inhibitor (EDTA) used in the current work acts as the electrons donor and the AA6061 hybrid composite surface as the acceptor. The EDTA molecules adsorb onto the hybrid composite surface and thus controls its corrosion. Mullikan's population analysis helps to identify the adsorption sites of EDTA. Generally, the more negatively charged heteroatoms have adsorbed on the metal surface by donor-acceptor mode of interactions [45]. It is clear from Table 7 that atoms such as O14, O15, O16, O17, O18, O19, O20, N3, N4 have higher charge densities and can therefore easily donate electrons [46, 47]. Hence, these O and N atoms in EDTA act as active centres, which strongly interact and result in the composite surface's protective film formation. Now, EDTA can exit in the fully protonated form ($H_6Y^{2+}$) in a very acidic medium like the one used in the current work (0.5M HCl). Hence, the DFT investigation of the protonated EDTA was also carried out. Fig. 9 (a) & (b) represents the optimized molecular structures of neutral and protonated EDTA. Similarly the Fig. 10 (a) & (b) depicts the HOMO of neutral and protonated EDTA. Fig. 11 (a) & (b) indicates the LUMO of neutral and protonated EDTA.

**Table 7**. Mulliken Charges of EDTA.

| Mulliken Charges on atom | | |
|---|---|---|
| **Atom** | **Neutral EDTA** | **Protonated EDTA** |
| N3 | -0.4154 | -0.4634 |
| N4 | -0.4265 | -0.4754 |
| O13 | -0.4812 | -0.4181 |
| O14 | -0.4642 | -0.4911 |
| O15 | -0.4817 | -0.5027 |
| O16 | -0.4602 | -0.3591 |
| O17 | -0.4847 | -0.4165 |
| O18 | -0.4825 | -0.4902 |
| O19 | -0.4741 | -0.4365 |
| O20 | -0.4605 | -0.4366 |

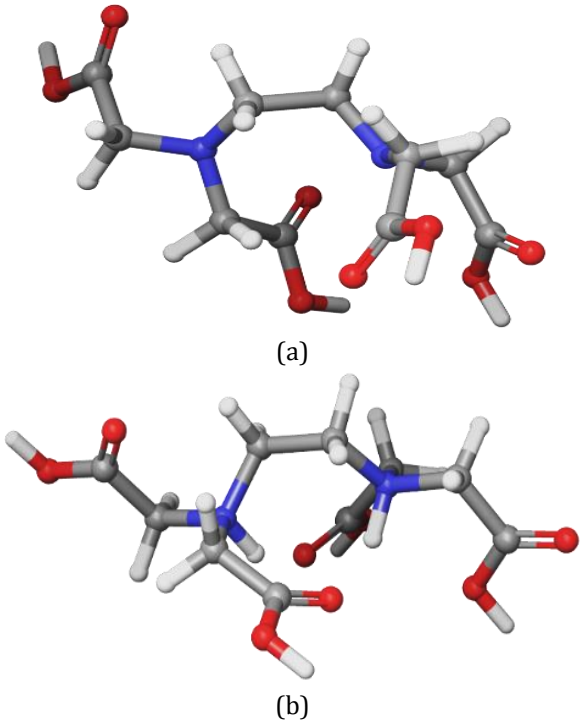

**Fig. 9.** Optimized molecular structures of (a) neutral and (b) protonated EDTA.

The quantum chemical parameters calculated using the following relations: [48, 49]

EHOMO is related to $I$ (Ionization potential), while ELUMO to $A$ (Electron affinity), as follows:

$$I = -E_{HOMO}\,. \tag{18}$$

$$A = -E_{LUMO}\,. \tag{19}$$

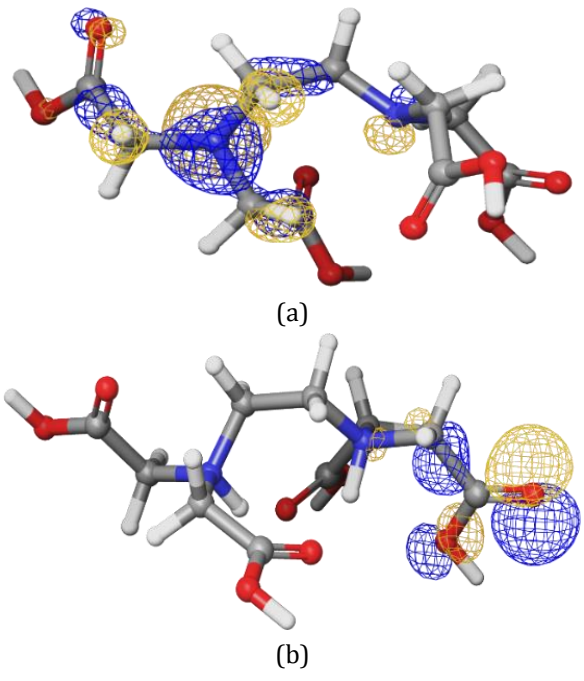

**Fig. 10.** HOMO of (a) neutral and (b) protonated EDTA.

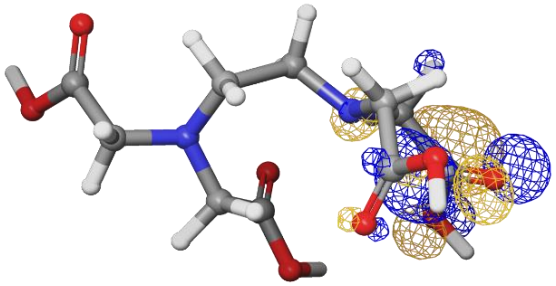

(a)

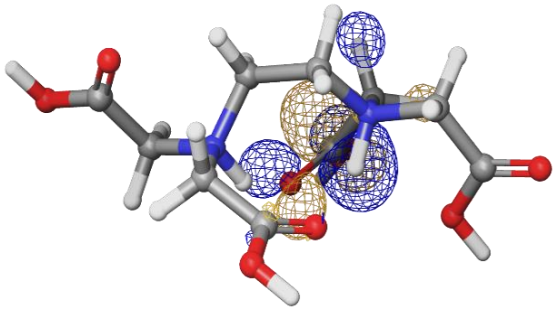

(b)

**Fig. 11.** LUMO of (a) neutral and (b) protonated EDTA.

The electronegativity ($\chi$) and the hardness ($\eta$) values were obtained using Eq. (20) and (21), respectively.

$$\chi = \frac{I+A}{2} . \quad (20)$$

$$\eta = \frac{I-A}{2} . \quad (21)$$

The number of electrons transferred electrons ($\Delta N$) has computed from Eq. (22):

$$\Delta N = \frac{\chi_{Al}-\chi_{EDTA}}{2(\eta_{Al}+\eta_{EDTA})} . \quad (22)$$

Where $\chi_{Al}$ and $\chi_{EDTA}$ is the electronegativity of Al and EDTA, respectively, $\eta_{Al}$ and $\eta_{EDTA}$ is the hardness of Al and EDTA. The softness value was obtained from the relation,

$$\sigma = \frac{1}{\eta} . \quad (23)$$

The quantum chemical parameters obtained have presented in Table 8.

**Table 8**. Quantum chemical parameters for EDTA.

| Parameters | Neutral EDTA | Protonated EDTA |
|---|---|---|
| $E_{HOMO}$ | -5.8918 | -14.341 |
| $E_{LUMO}$ | -0.6132 | -7.7416 |
| Band gap ($E_g$) | 5.2786 | 6.5994 |
| Ionization potential (I) | 5.8918 | 14.341 |
| Electron affinity (A) | 0.6132 | 7.741 |
| Electronegativity (χ) | 3.0275 | 11.041 |
| Global hardness (η) | 2.8643 | 3.2997 |
| Global softness (σ) | 0.3491 | 0.3030 |
| Fractions of electron transferred (ΔN) | 0.2186 | -1.0245 |

The $E_{HOMO}$, $E_{LUMO}$, $E_g$, and $\Delta N$ values play a significant role in predicting the inhibitor species' chemical reactivity and stability [50]. A higher value of $E_{HOMO}$ shows the tendency of the molecule to release electrons, whereas the lower $E_{LUMO}$ indicates the tendency to receive electrons [51, 26]. The protonated EDTA has shown a much higher $E_{HOMO}$ value (Table 8) than neutral EDTA, suggesting the former's higher electron-donating property. Hence, this supports the formation of coordinate type bonding. Further, the lower $E_{LUMO}$ value of neutral EDTA showed a higher tendency to accept electrons, supporting back bonding. A positive value for $\Delta N$ reveals that the inhibitor molecule can readily share its electrons and reverse for a negative value [52]. $\Delta N$ value is positive (0.2186) for neutral EDTA, while it is negative for protonated EDTA (-1.0245). This reveals the neutral EDTA's electron donating and the electron accepting nature of protonated EDTA. The lower the $E_g$ value, the higher is the reactivity of the inhibitor molecules that provide good inhibition activity [53]. The $E_g$ for neutral EDTA is lower than that of protonated EDTA (Table 8), and hence neutral EDTA becomes more reactive.

According to HSAB theory, a molecule's inhibition activity influenced by its global hardness and softness values. A soft molecule shows a higher affinity to interact compared to a hard molecule. The lower global hardness and higher global softness values for neutral EDTA than protonated EDTA reveal the neutral EDTA's better inhibition activity. Further, the lower values of $E_g$, and χ, while a higher value of $\Delta N$ for neutral EDTA, indicate its more significant contribution towards inhibition activity than protonated EDTA, based on its better ability to donate electrons [54].

## 4. CONCLUSION

- EDTA is an excellent eco-friendly inhibitor for AA6061 hybrid composite in 0.5M HCl medium.
- The results of PDP revealed the mixed inhibitor behaviour of EDTA.
- Inhibition performance of EDTA increased on increasing its concentration and displayed a moderate *IE* of 84% at 1.074 mM and 303K.
- The inhibition mechanism followed mixed adsorption of EDTA mainly with physisorption and the adsorption model of Langmuir isotherm.

- SEM and AFM analyses validated the deposition of defensive coating of EDTA on the hybrid composite surface.
- The experimental results obtained for the AA6061 hybrid composite-EDTA system match with those obtained by quantum chemical calculations.

## Acknowledgment

J.D.E. Robledo gratefully acknowledged the Manipal Institute of Technology, Manipal Academy of Higher Education, Manipal, for providing the laboratory facilities.

## REFERENCES

[1] J. Fan, J. Njuguna, *An introduction to lightweight composite materials and their use in transport structures*, in J. Njuguna (Ed.): Lightweight composite structures in Transport, Design, Manufacturing, Analysis, and Performance, Woodhead Publishing, Elsevier Ltd, pp. 3–34, 2016 doi: 10.1016/B978-1-78242-325-6.00001-3

[2] D. Gay, *Composite Materials: Design and Applications*, New York: CRC Press, Taylor & Francis Group, 2014.

[3] M. Uthayakumar, S. Aravindan, K. Rajkumar, *Wear performance of Al–SiC–B4C hybrid composites under dry sliding conditions*, Materials and Design, vol. 47, pp. 456–464, 2013, doi: 10.1016/j.matdes.2012.11.059

[4] J. O'M. Bockris, L.V. Minevski, *On the mechanism of the passivity of aluminium and aluminium alloys*, Journal of Electroanalytical Chemistry, vol. 349, iss. 1-2, pp. 375-414, 1993, doi: 10.1016/0022-0728(93)80186-L

[5] M. Patel, B. Pardhi, M. Pal, M.K. Singh, *SiC particulate reinforced Aluminium metal matrix composite*, Advanced journal of graduate research, vol. 5, no. 1, pp. 8-15, 2019, doi: 10.21467/ajgr.5.1.8-15

[6] L. Poovazhagan, K. Kalaichelvan, A. Rajadurai, V. Senthilvelan, *Characterization of hybrid silicon carbide and boron carbide nanoparticles-reinforced aluminium alloy composites*, Procedia Engineering, vol. 64, pp. 681–689, 2013, doi: 10.1016/j.proeng.2013.09.143

[7] P.K. Rohatgi, *Aqueous Corrosion of Metal Matrix Composites,* in A. Kelly, C. Zweben (Ed.): Comprehensive composite materials, pp. 481-500, 2000, doi: 10.1016/B0-08-042993-9/00017-6

[8] A.J. Trowsdale, B. Noble, S.J. Haris, I.S.R. Gibbins, G.E. Thomson, G.C. Wood, *The influence of silicon carbide reinforcement on the pitting behavior of aluminium*, Corrosion Science, vol. 38, iss. 2, pp. 177–191, 1996. doi: 10.1016/0010-938X(96)00098-4

[9] B. Bobic., S. Mitrovic, M. Babic, I. Bobic, *Corrosion of metal-matrix composites with aluminium alloy substrate*, Tribology in industry, vol. 32, no. 1, pp. 3-11, 2010.

[10] A. Pardo, M.C. Merino, M.D. Lopez, F. Viejo, M. Carboneras, S. Merino, *Influence of reinforcement grade and matrix composition on corrosion resistance in cast aluminium matrix composites (A3xx.x/SiCp) on 80% HR*, Materials and Corrosion, vol. 54, iss. 5, pp. 311-317, 2003. doi: 10.1002/maco.200390070

[11] K. Xhanari, M. Finsgar, *Organic corrosion inhibitors for aluminium and its alloys in acid solutions: a review*, RSC Advances, vol. 6, iss. 67, pp. 62833-62857, 2016, doi: 10.1039/c6ra11818f

[12] P. Shetty, Schiff bases: *An overview of their corrosion inhibition activity in acid media against mild steel*, Chemical Engineering Communication, vol. 207, iss. 7, pp. 985–1029, 2020, doi: 10.1080/00986445.2019.1630387

[13] R. Rosliza, W.B. Wan Nik, S. Izman, Y. Prawoto, *Anti corrosive properties of natural honey on Al-Mg-Si alloy in seawater*, Current Applied Physics, vol. 10, iss. 3, pp. 923-929, 2010, doi: 10.1016/j.cap.2009.11.074

[14] W.B. Wan Nik, F. Zulkifli, O. Sulaiman, K.B. Samo, R. Rosliza, *Study of Henna (Lawsonia inermis) as natural corrosion inhibitor for aluminium alloy in seawater*, IOP Conference Series: Materials Science and Engineering, vol. 36, pp. 1-8, 2012, doi: 10.1088/1757-899X/36/1/012043

[15] K.M. Zohdy, *Surface protection of carbon steel in acidic solution using ethylene diamine tetra acetic disodium salt*, International Journal of Electrochemical Science, vol.10, pp. 414 – 431, 2015.

[16] R.E. Azooz, *EDTA as a corrosion inhibitor for Al in 0.5 M HCl*: *adsorption, thermodynamic and theoretical study*, Journal of Electrochemical Science and Engineering, vol. 6, iss. 3, pp. 235-251, 2016, doi: 10.5599/jese.300

[17] S.S. Sharma, K. Jagannath, P.R. Prabhu, Gowri Shankar, S. R. Harisha, A. Kini, *Metallography & bulk hardness of artificially aged Al6061-B4C-SiC stir cast hybrid composites*, Materials Science Forum, vol. 880, pp 140-143, 2017, doi: 10.4028/www.scientific.net/MSF.880.140

[18] S.A. Umoren, I.B. Obot, E.E. Ebenso, N.O. Obi-Egbedi, *The Inhibition of aluminium corrosion in hydrochloric acid solution by exudate gum from*

*Raphia hookeri*, Desalination, vol. 247, iss. 1-3, pp. 561–572, 2009, doi: 10.1016/j.desal.2008.09.005

[19] C. Lee, W. Yang, R.G. Parr, *Development of the Colle-Salvetti correlation-energy formula into a functional of the electron density*. Physics Review Condense Mater B, vol. 37, iss. 2-15, pp. 785–789, 1998, doi: 10.1103/PhysRevB.37.785

[20] P.O. Ameh, N.O. Eddy, *Commiphora pedunculata gum as a green inhibitor for the corrosion of aluminium alloy in 0.1 M HCl*, Research on Chemical Intermediates, vol. 40, pp. 2641-2649, 2014, doi: 10.1007/s11164-013-1117-0

[21] M.G. Fontana, *Corrosion Engineering*, New York: McGraw-Hill, 1987.

[22] U.A. Kini, Prakash Shetty, S.D. Shetty, A. Isloor, R. Herle, *The inhibition action of ethyl-2-phenyl hydrozono-3-oxobutyrate on the corrosion of 6061Al alloy/$SiC_p$ composite in hydrochloric acid medium*, Journal of Chilean Chemical Society, vol. 55, no. 1, pp. 56-60, 2010, doi: 10.4067/S0717-97072010000100014

[23] S.S. Abd El Rehim, H.H. Hassan, M.A. Amin, *The corrosion inhibition study of sodium dodecylbenzene sulphonated to aluminium and its alloys in 1.0 M HCl solution*, Materials Chemistry and Physics, vol. 78, iss. 2, pp. 337–348, 2002, doi: 10.1016/S0254-0584(01)00602-2

[24] K.F. Khaled, M.M. Al-Qahtani, *The inhibitive effect of some tetrazole derivatives towards Al corrosion in acid solution: Chemical, electrochemical and theoretical studies*, Materials Chemistry and Physics, vol. 113, iss. 1, pp. 150-158, 2009, doi: 10.1016/j.matchemphys.2008.07.060

[25] B.P. Charitha, P. Rao, *Protection of 6061 Al-15%(v) SiC(P) composite from corrosion by a biopolymer and surface morphology studies*, Protection of Metals and Physical Chemistry of Surfaces, vol. 52, iss. 4, pp. 704–713, 2016, doi: 10.1134/S2070205116040079

[26] M. Abdallah, *Antibacterial drugs as corrosion inhibitors for corrosion of aluminium in hydrochloric solution*, Corrosion Science, vol. 46, iss. 8, pp. 1981-1996, 2004, doi: 10.1016/j.corsci.2003.09.031

[27] E.E. Oguzie, *Corrosion inhibition of aluminium in acidic and alkaline media by Sansevieria trifasciata extract*, Corrosion Science, vol. 49, iss. 3, pp. 1527-1539, 2007, doi: 10.1016/j.corsci.2006.08.009

[28] M. Schorr, J. Yahalom, *The significance of the energy of activation for the dissolution reaction of metal in acids,* Corrosion Science, vol. 12, iss. 11, pp. 867-868, 1972, doi: 10.1016/S0010-938X(72)80015-5

[29] M.M. Osman, R.A. El-Ghazawy, A.M. Al-Sabagh, *Corrosion inhibitor of some surfactants derived from maleic-oleic acid adduct on mild steel in 1 M $H_2SO_4$*, Materials Chemistry and Physics, vol. 80, iss. 1, pp. 55-62, 2003, doi: 10.1016/S0254-0584(01)00588-0

[30] F. Mansfeld, *Corrosion Mechanism*, New York: CRC Press, 1987.

[31] J.O.M. Bockris, A.K.N. Reddy, *Modern Electrochemistry*, vol. 2, New York: Springer, 1977.

[32] S.S. Shivakumar, K.N. Mohana, *Studies on the inhibitive performance of cinnamomum zeylanicum extracts on the corrosion of mild steel in hydrochloric acid and sulphuric acid media*, Journal of Materials and Environment Science, vol. 4, iss. 3, pp. 448-459, 2013.

[33] E. Bayol, K. Kayakırılmaz, M. Erbil, *The inhibitive effect of hexamethylenetetramine on the acid corrosion of steel*, Materials Chemistry and Physics, vol. 104, iss. 1, pp. 74-82, 2007, doi: 10.1016/j.matchemphys.2007.02.073

[34] N. Soltani, M. Behpour, S.M. Ghoreishi, H. Naeimi, *Corrosion inhibition of mild steel in hydrochloric acid solution by some double Schiff bases*, Corrosion Science, vol. 52, iss. 4, pp. 1351-1361, 2010, doi: 10.1016/j.corsci.2009.11.045

[35] L.A. Nnanna, B.N. Onwuagba, I.M. Mejeha, K.B. Okeoma, *Inhibition effects of some plant extracts on the acid corrosion of aluminum alloy*, African Journal of Pure and Applied Chemistry, vol. 4, no. 2, 11–16, 2010, doi: 10.5897/AJPAC.9000079

[36] P.P. Kumari, P. Shetty, S.A. Rao, D. Sunil, T. Vishwanath, *Synthesis, character-rization and anticorrosion behaviour of a novel hydrazide derivative on mild steel in hydrochloric acid medium*, Bulletin of Material Science, vol. 43, pp. 1-14, 2020, doi: 10.1007/s12034-019-1995-x

[37] E. Ech-chihbi, M.E. Belghiti, R. Salim, H. Oudda, M. Taleb, N. Benchat, B. Hammouti, F. El-Hajjaji, *Experimental and computational studies on the inhibition performance of the organic compound 2-phenylimidazo [1,2-a]pyrimidine-3-carbal- dehyde against the corrosion of carbon steel in 1.0M HCl solution*, Surfaces and Interfaces, vol. 9, pp. 206–217, 2017, doi: 10.1016/j.surfin.2017.09.012

[38] M. Metikos-Hukovic, R. Babic, Z. Grubac, *Corrosion protection of aluminium in acidic chloride solutions with nontoxic inhibitors*, Journal of Applied Electrochemistry, vol. 28, pp. 433-439, 1998. doi: 10.1023/A:1003200808093

[39] E.A. Noor, *Evaluation of inhibitive action of some quaternary N-heterocyclic compounds on the corrosion of Al–Cu alloy in hydro chlo- ric acid*, Material Chemistry and Physics, vol. 114, iss. 2-3, 533-541, 2009, doi: 10.1016/j.matchemphys.2008.09.065

[40] G.M. Pinto, J. Nayak, A. Nityananda Shetty, *Corrosion inhibition of 6061 Al–15 vol. pct. $SiC_{(p)}$ composite and its base alloy in a mixture of sulphuric acid and hydrochloric acid by 4-(N, N-dimethyl amino) benzaldehyde thiosemicarbazone*, Material Chemistry and Physics, vol. 125, iss. 3, pp. 628–640, 2011, doi: 10.1016/j.matchemphys.2010.10.006

[41] P.P. Kumari, P. Shetty, Nagalaxmi, D. Sunil, *Effect of cysteine as environmentally friendly inhibitor on AA6061-T6 corrosion in 0.5 M HCl: Electro- chemical and Surface Studies*, Surface Engineering and Applied Electrochemistry, vol. 56, no. 5, pp. 624-634, 2020, doi: 10.3103/S1068375520050087

[42] G. Bereket, A. Pinarbsi, *Electrochemical thermodynamic and kinetic studies of the behaviour of aluminium in hydrochloric acid containing various benzotriazole derivatives*, Corrosion Engineering Science and Technology, vol. 39, iss. 4, pp. 308-312, 2004, doi: 10.1179/174327804X13136

[43] G.M. Treacy, A.L. Rudd, C.B. Breslin, *Electrochemical behaviour of aluminium in the presence of EDTA-containing chloride solutions*, Journal of Applied Electro chemistry, vol. 30, 675-683, 2000, doi: 10.1023/A:1003945214539

[44] N. Hackerman, E.S. Jr Snavely, J.S. Jr Payne, *Effect of anions on corrosion inhibition by organic compounds*, Journal of Electro chemical Society, vol. 113, no. 7, pp. 671-686, 1966, doi: 10.1149/1.2424089

[45] O. Senhaji, R. Taouil, M.K. Skalli, M. Bouachrine, B. Hammouti, M. Hamidi, *Experimental and theoretical study for corrosion inhibition in normal hydrochloric acid solution by some new phosphonated compounds*, International Journal of Electrochemical Science, vol. 6, pp. 6290–6299, 2011.

[46] I. Lukovits, E. Kalman, F. Zucchi, *Corrosion Inhibitors-Correlation between electronic structure and efficiency*, Corrosion, vol. 57, iss. 1, pp. 3-8, 2001, doi: 10.5006/1.3290328

[47] A.Y. Musa, A.H. Kadhum, A. Mohamad, M.S. Takriff, *Experimental and theoretical study on the inhibition performance of triazole compounds for mild steel corrosion*, Corrosion Science, vol. 52, iss. 10, pp. 3331-3340, 2010, doi: 10.1016/j.corsci.2010.06.002

[48] R.G. Pearson, *Absolute electronegativity and hardness: Application to inorganic chemistry*, Inorganic Chemistry, vol. 27, iss. 4, pp. 734-740. 1988, doi: 10.1021/ic00277a030

[49] Z. Chang-Guo, J.A. Nichols, D.A. Dixon, *Ionization Potential, Electron Affinity, Electronegativity, Hardness, and Electron Excitation Energy: Molecular Properties from Density Functional Theory Orbital Energies*, Journal of Physical Chemistry A, vol. 107, iss. 20, pp. 4184-4195, 2003, doi: 10.1021/jp0225774

[50] Z. Salarvand, M. Amirnasr, M. Talebian, K. Raeissi, S. Meghdadi, *Enhanced corrosion resistance of mild steel in 1M HCl solution by trace amount of 2-phenyl-benzothiazole derivatives: Experimental, Quantum Chemical Calculations and Molecular Dynamics (MD) Simulation Studies*. Corrosion Science, vol. 114, pp. 133–145, 2017, doi: 10.1016/j.corsci.2016.11.002

[51] W. Li, X. Zhao. Liu, J. Deng, B. Hou, *Investigation on the corrosion inhibitive effect of 2H-pyrazole-triazole derivatives in acidic solution*, Material Corrosion, vol. 60, iss. 4, pp. 287–293, 2009, doi: 10.1002/maco.200805081

[52] S. Dahiya, N. Saini, N. Dahiya, H. Lgaz, R. Salghi, S. Jodeh, S. Lata, *Corrosion inhibition activity of an expired antibacterial drug in acidic media amid elucidate DFT and MD Simulations*, Portugalai Electrochemical Acta, vol. 36, iss. 3, pp. 213–230, 2018, doi: 10.4152/pea.201803213

[53] V. Srivastava, J. Haque, C. Verma, P. Singh, H. Lgaz, R. Salghi, M.A. Quraishi, *Amino acid based imidazolium Zwitterions as novel and green corrosion inhibitors for mild steel: Experimental, DFT and MD Studies*, Journal of Molecular Liquids, vol. 244, pp. 340–352, 2017, doi: 10.1016/j.molliq.2017.08.049

[54] J. Haque, C. Verma, V. Srivastava, W.B. Wan Nik, *Corrosion inhibition of mild steel in 1M HCl using environmentally benign Thevetia peruviana flower extracts*, Sustainable Chemistry and Pharmacy, vol. 19, 100354, 2021. doi: 10.1016/j.scp.2020.100354